Study of the arrival directions of ultra-high-energy cosmic rays detected by the Pierre Auger Observatory

Piera L. Ghia for the Pierre Auger Collaboration*

**IPN, Orsay, IN2P3/CNRS and Univ. Paris Sud and Paris Saclay*

Study of the arrival directions of ultra-high-energy cosmic rays detected by the Pierre Auger Observatory

"…What extraordinary processes are capable of accelerating particles to such enormous energies? In the hope of finding clues to the solution, physicists would like to know whether the most energetic particles come from all directions or only from certain regions of the sky…"

Bruno Rossi, 1964

Piera L. Ghia for the Pierre Auger Collaboration*

**IPN, Orsay, IN2P3/CNRS and Univ. Paris Sud and Paris Saclay*

Auger and directional analyses: a ≈15 years thread

Search for anisotropies in the distribution of the arrival directions:
a natural and central quest since the start of the data taking.

Two lines of analyses pursued with increasing statistics:

At “low” energies (O(EeV): “Large” scale studies

- **Aim**: studying the evolution of the amplitude and direction of anisotropy vs energy to identify their origin, galactic vs extra-galactic, and the transition from one to the other. Propagation and/or source distributions may imprint large-scale anisotropy
- **Method**: Rayleigh analysis in right ascension
- **Challenge**: Control of the exposure and of the counting rate down to < % level

At the highest energies: “Small” scale studies

- **Aim**: reducing the “horizon” and exploiting the high rigidity to probe the sources more directly. Only few are capable of accelerating at UHE. Inhomogeneities in their spatial distribution may imprint anisotropy on a smaller scale
- **Method**: Comparison of UHECR arrival directions with astronomical objects
- **Challenge**: control of the exposure and trial factors (angle, energy…)

Common to both are the data, their treatment, their understanding and their control

From the surface detector: ≈ 100% duty cycle

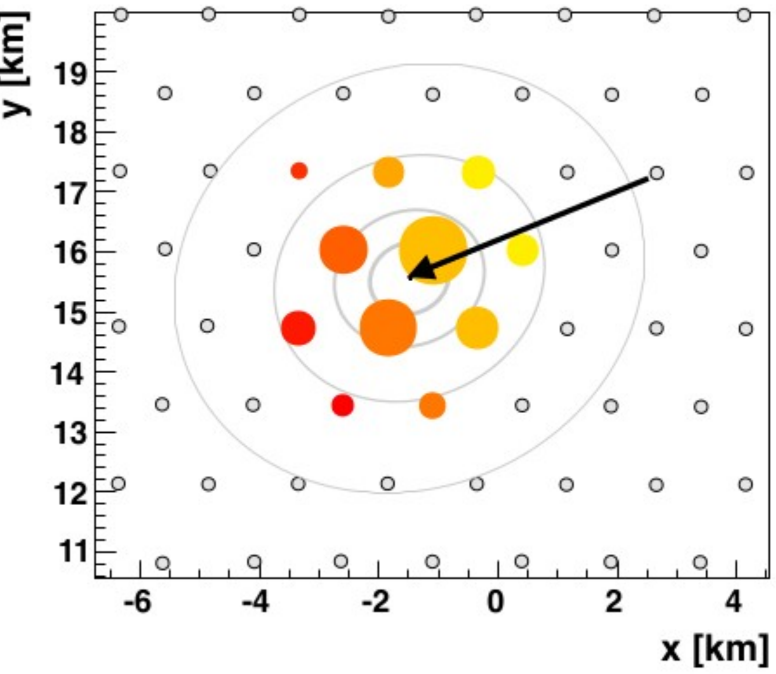

+

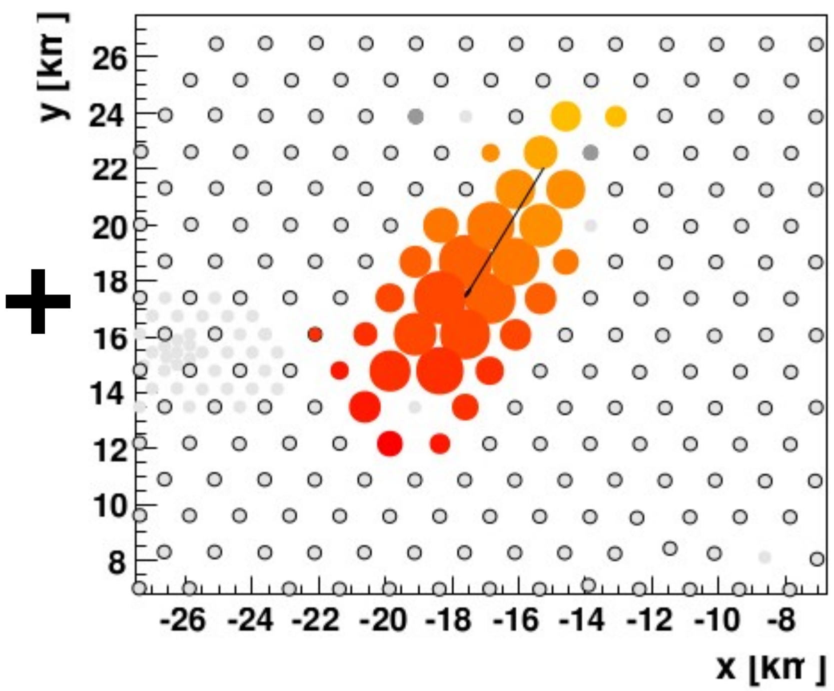

=

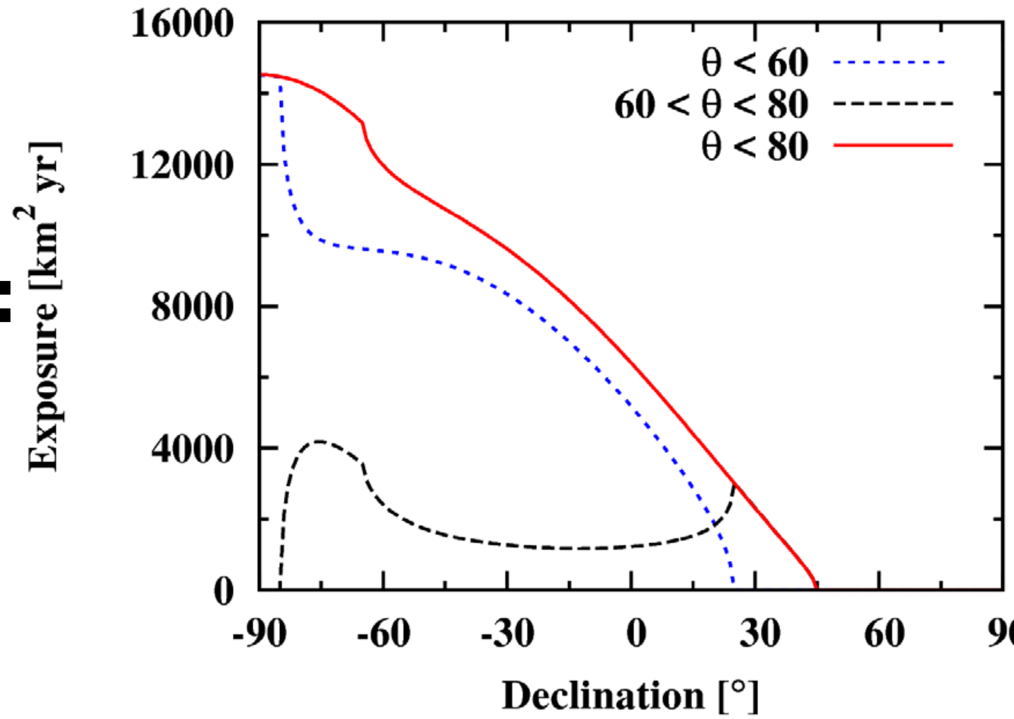

Vertical events
$\vartheta < 60^\circ$

Horizontal events
$60^\circ < \vartheta < 80^\circ$

85% of the sky covered

Different reconstructions, but similar resolutions:

≈ 1° for the arrival direction, 12%-16% for the energy.

Same energy scale, calibrated with the fluorescence detector:

14% systematic uncertainty.

The data: systematic effects

Correction for atmospheric and geomagnetic effects

[Auger Coll. JINST 12 P02006 (2017), JCAP 11 (2011) 022]

Atmospheric effects:
Impact on the absorption of em component due to P and T variations.
Energy correction on vertical events.
No correction on horizontal ones (mostly muons).

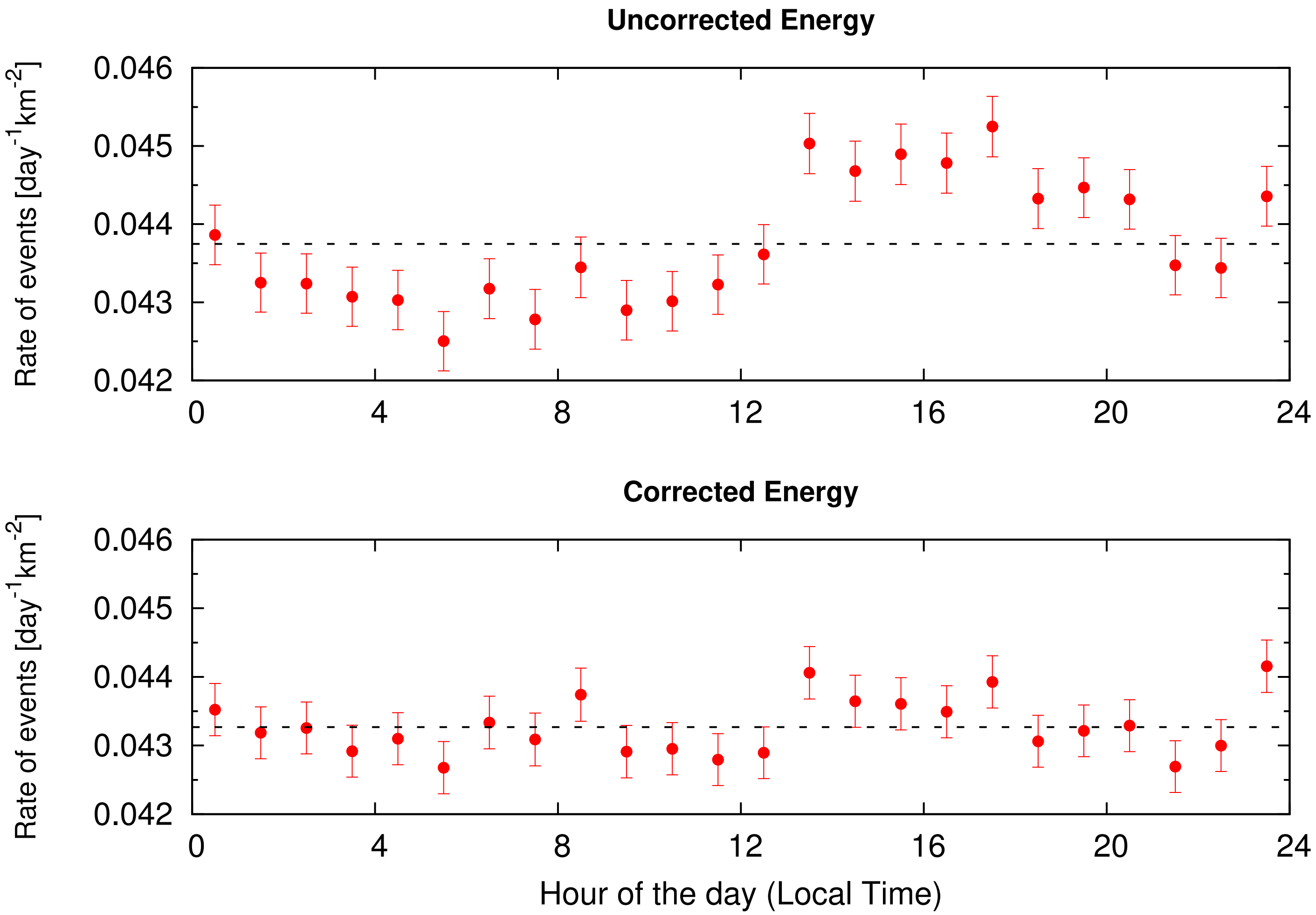

Uncorrected:
± 1.7% variations in solar time

Corrected:
Amplitude 0.5 ± 0.4%

Geomagnetic effects:

Impact on the circular symmetry of the shower. Larger effect at larger angles.
If uncorrected, it would induce modulation in azimuthal angle (0.7%).
Energy correction on both vertical and horizontal events.

The exposure: systematic effects

Purely geometrical exposure controlled at second level

[Auger Coll. NIM A613 (2010) 29]

Geometrical exposure:

Fiducial cuts to ensure containment.

Events used only above the energy yielding full efficiency (E > 4 EeV)

Exposure = sum of active "elementary cells"/sec integrated over time

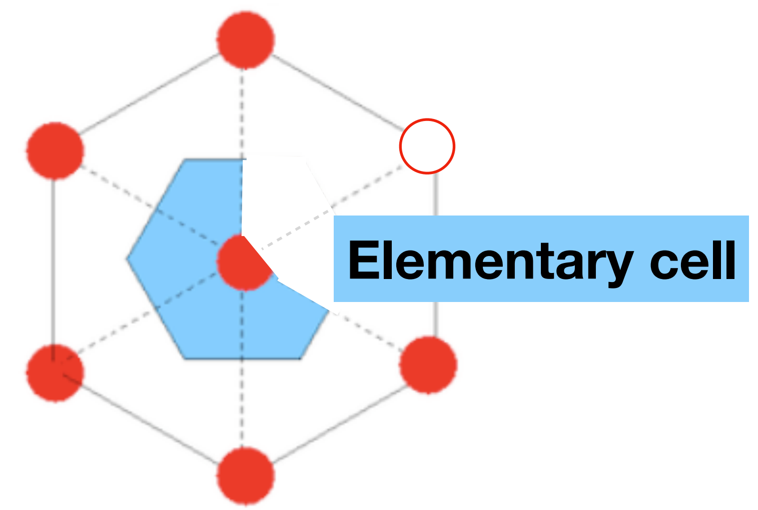

Control of the exposure:

The number of "cells" is not constant (maintenance, power, communications…)

Amplitude of the modulation : < 0.6%

Small, yet we account for that

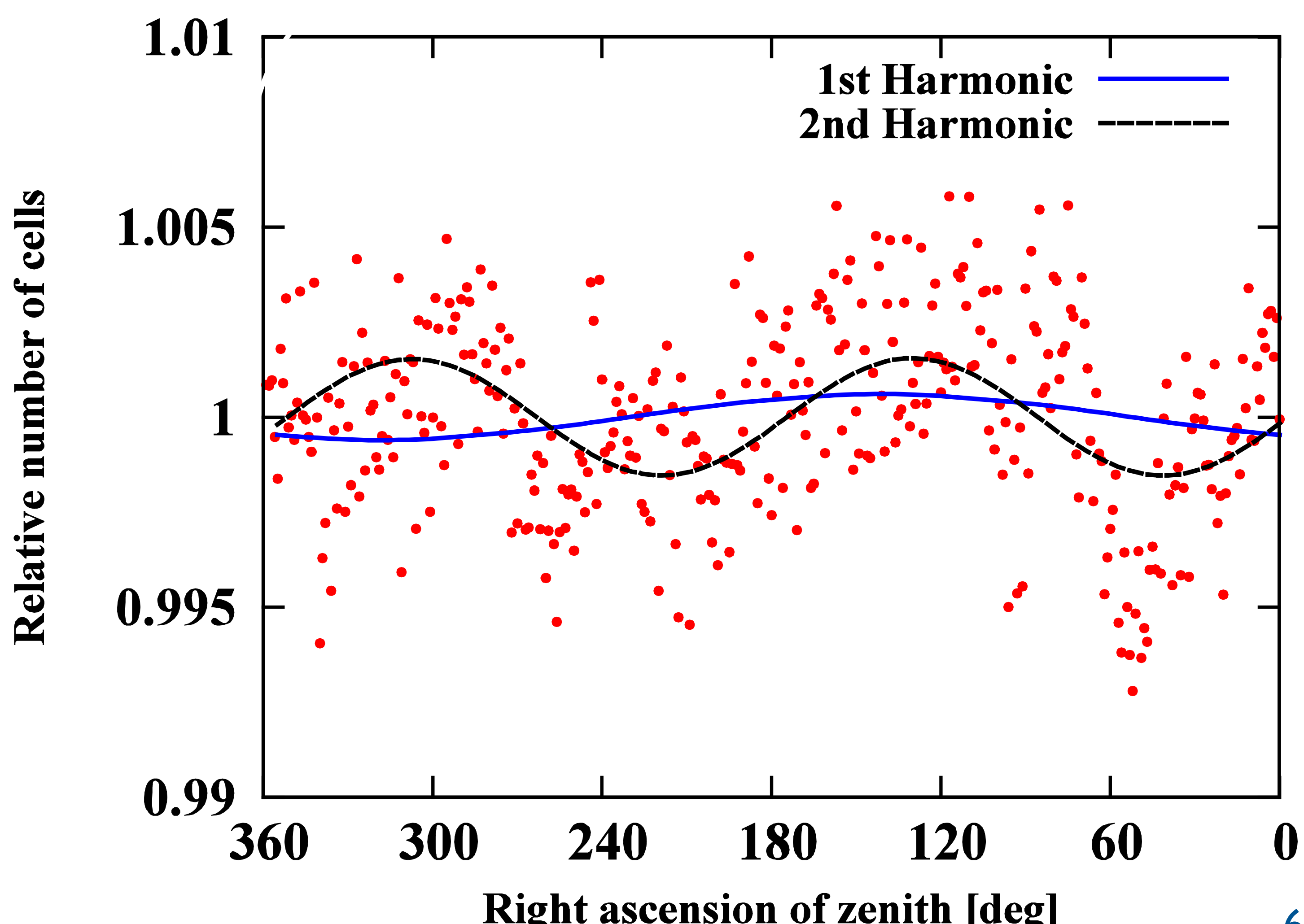

Large-scale analysis: the method

Harmonic analysis in right ascension

[J. Linsley PRL 34 (1975) 1530]

First-harmonic components

$$a_\alpha = \frac{2}{\mathcal{N}} \sum_{i=1}^{N} w_i \cos \alpha_i$$

$$b_\alpha = \frac{2}{\mathcal{N}} \sum_{i=1}^{N} w_i \sin \alpha_i$$

Modified to include weights w_i accounting for exposure variations and for the slight tilt (0.2°) of the array

Amplitude and phase

$$r_\alpha = \sqrt{a_\alpha^2 + b_\alpha^2}$$

$$\tan \varphi_\alpha = \frac{b_\alpha}{a_\alpha}$$

Chance probability for an amplitude being larger than that observed:

cumulative distribution function of the Rayleigh distribution

$$P(r_\alpha) = \exp(-\mathcal{N} r_\alpha^2/4)$$

Large-scale analysis: first harmonic in RA

First harmonic analysis applied in two energy bins (4-8 EeV and > 8 EeV)

[Auger Coll. Science 357 (2017) 1266]

		Harmonic	Components		Amplitude	Phase	Probability
Energy [EeV]	events	k	a_k^α	b_k^α	r_k^α	φ_k^α [°]	$P(\geq r_k^\alpha)$
4 - 8	81,701	1	0.001 ± 0.005	0.005 ± 0.005	0.005	80 ± 60	0.60
≥ 8	32,187	1	-0.008 ± 0.008	0.046 ± 0.008	0.047	100 ± 10	2.6×10^{-8}

4-8 EeV bin:
consistent with isotropy:
r < 0.012 @ 95% c.l.

> 8 EeV bin: r = 0.047 ± 0.008
φ = 100˚±10˚
P(r) = 2.6 x 10^{-8} (5.6 s.d.)
Post-trial (two energy bins)*:
5.4 s.d.

E > 8 EeV

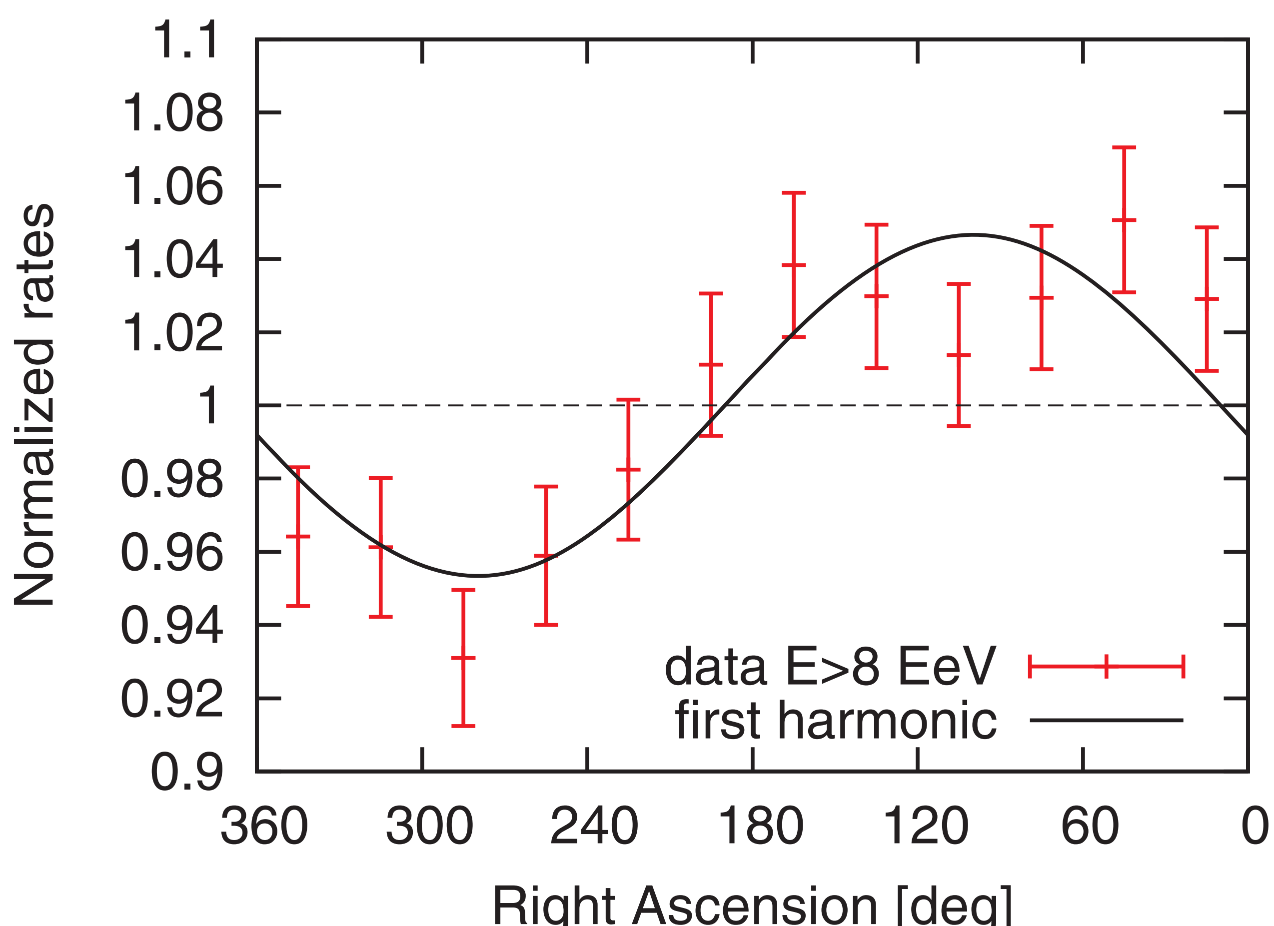

* Post-trial (six energy bins, as in APP, 34, 2011, 627)*: 5.2 s.d.

Large-scale analysis: sanity checks

First harmonic analysis in solar and antisidereal time
Evolution of the significance over time

First-harmonic amplitude in solar and anti-sidereal time not significant in any of the two energy bins

Energy	solar		anti-sidereal	
[EeV]	r_1	$P(\geq r_1)$	r_1	$P(\geq r_1)$
4 - 8	0.006	0.48	0.004	0.76
≥ 8	0.007	0.69	0.011	0.36

Significance of the first-harmonic amplitude in right ascension became larger as the exposure increased.
Cross-check with different fiducial cuts

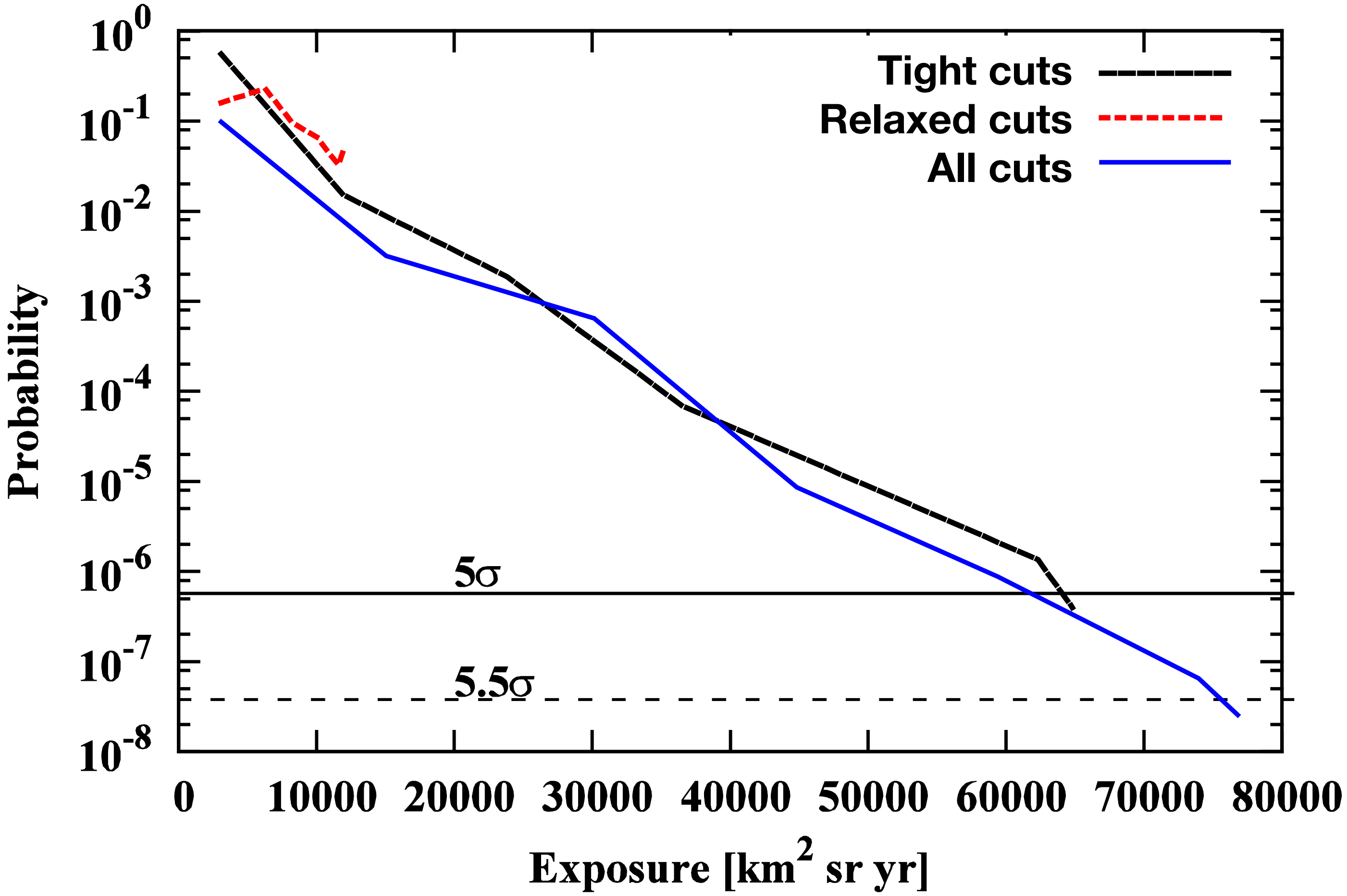

Large-scale analysis: reconstruction of the dipole

Harmonic analysis in RA:

Only sensitive to the anisotropy component orthogonal to the Earth's rotation axis

The distribution of the azimuth angles is in turn sensitive to the N/S component:

Harmonic analysis in azimuthal angles performed

Under the assumption that the anisotropy is purely dipolar, the first-harmonic coefficients in RA and azimuth are sufficient to reconstruct the dipole

Reconstruction of amplitudes

$$d_\perp \approx \frac{r_\alpha}{\langle \cos\delta \rangle}$$

$$d_z \approx \frac{b_\varphi}{\cos\ell_{\rm obs}\langle \sin\theta \rangle}$$

Reconstruction of directions

$$\alpha_{\rm d} = \varphi_\alpha$$

$$\tan\delta_{\rm d} = \frac{d_z}{d_\perp}$$

Large-scale analysis: reconstruction of the dipole

Amplitude: 6.5$^{+1.3}_{-0.9}$%

Right ascension: 100°±10°, Declination: -24°±13°

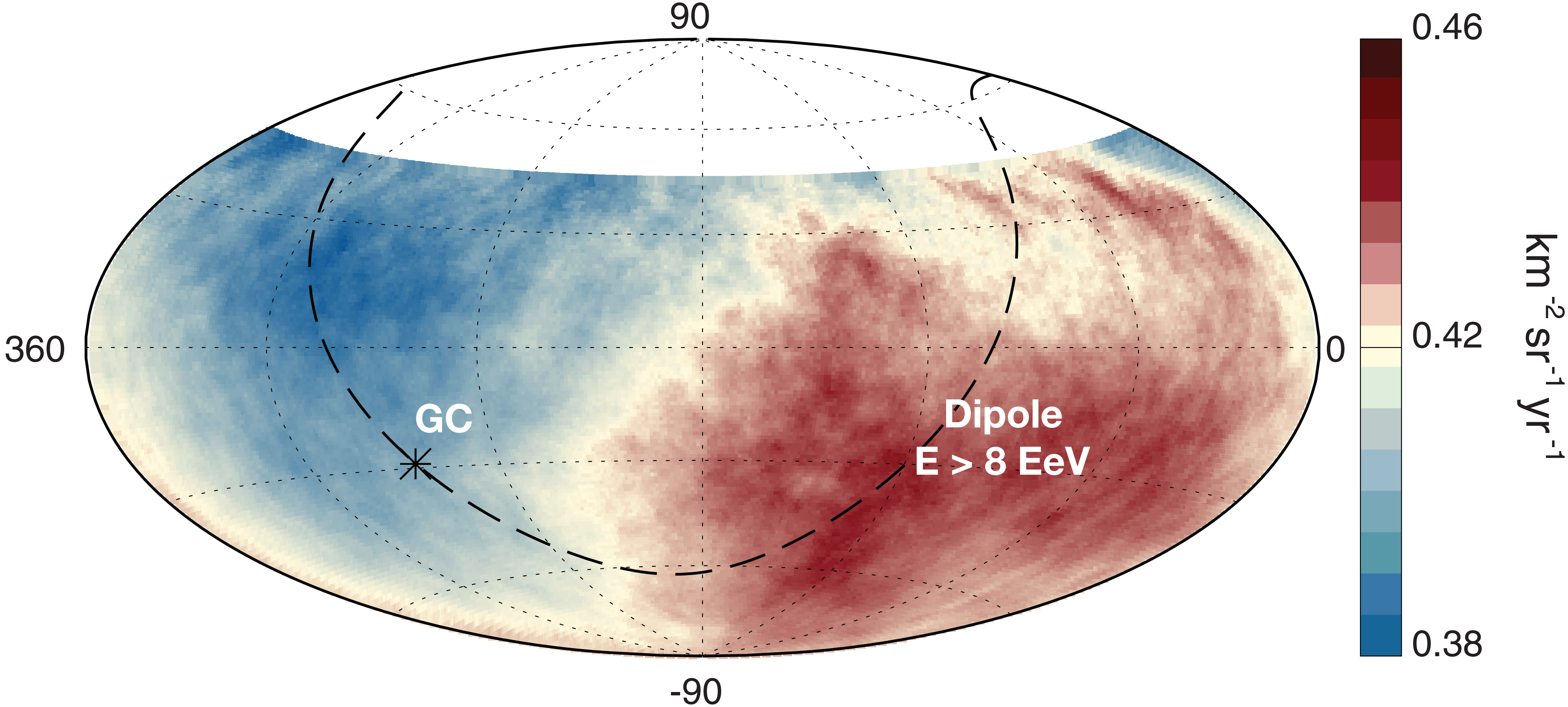

The direction of the dipole lies ≈ 125° from the Galactic Center

Origin hard to explain with a Galactic origin

Large-scale analysis: other studies

Second harmonic analysis applied in two energy bins (4-8 EeV and > 8 EeV)

[Auger Coll. arXiv 1808.03579, just accepted by ApJ]

		Harmonic	Components		Amplitude	Phase	Probability
Energy [EeV]	events	k	a_k^α	b_k^α	r_k^α	$\varphi_k^\alpha [^\circ]$	$P(\geq r_k^\alpha)$
4 - 8	81,701	1	0.001 ± 0.005	0.005 ± 0.005	0.005	80 ± 60	0.60
		2	-0.001 ± 0.005	0.001 ± 0.005	0.002	70 ± 80	0.94
≥ 8	32,187	1	-0.008 ± 0.008	0.046 ± 0.008	0.047	100 ± 10	2.6×10^{-8}
		2	0.013 ± 0.008	0.012 ± 0.008	0.018	21 ± 12	0.065

No statistically significant second harmonic in any of the two energy bin

E > 8 EeV

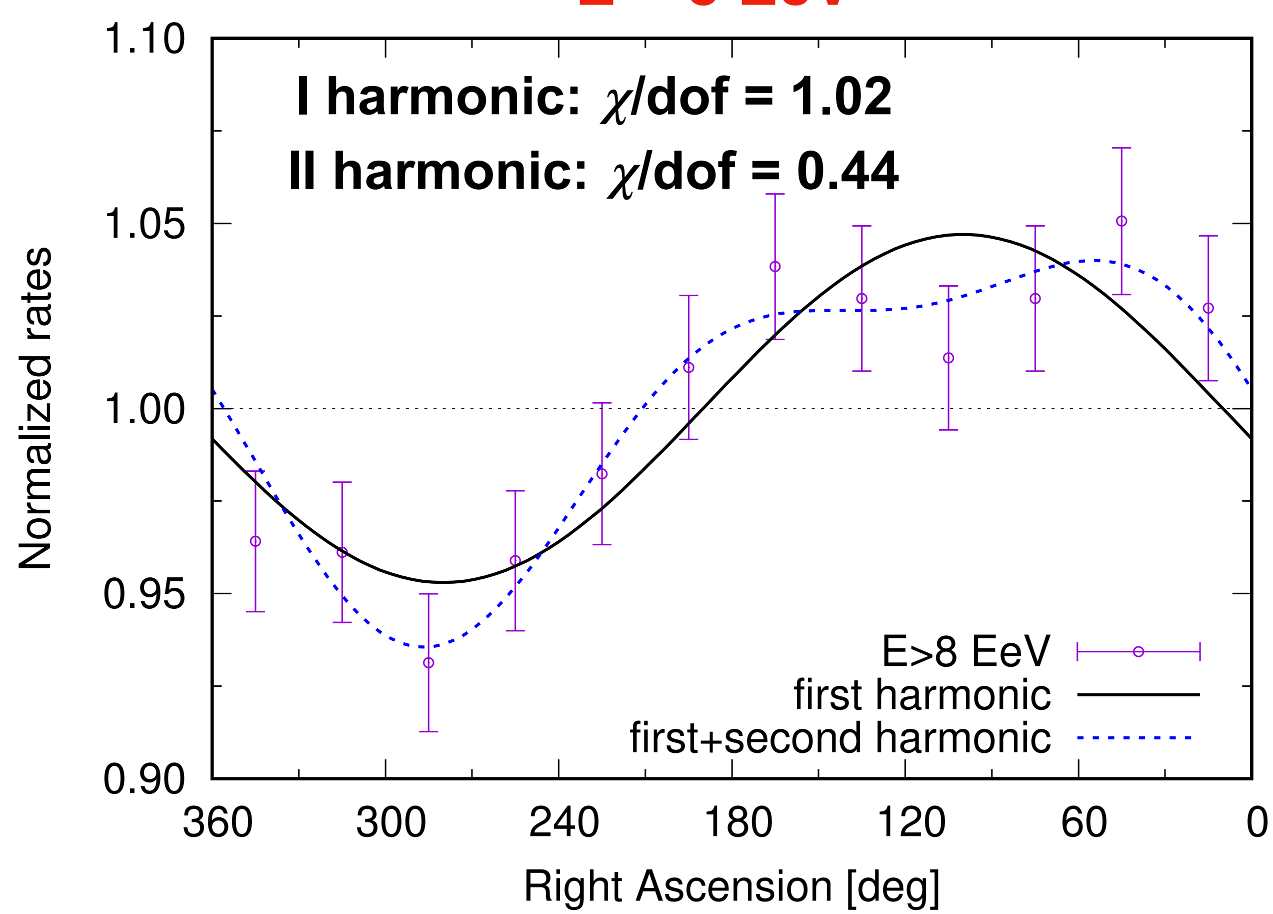

Large-scale analysis: other studies

Study of a possible evolution of the first harmonic in RA vs energy

[Auger Coll. arXiv 1808.03579, just accepted by ApJ]

Dividing the E > 8 EeV bin into three

Energy [EeV]	events	a_1^α	b_1^α	r_1^α	φ_1^α [°]	$P(\geq r_1^\alpha)$
8 - 16	24,070	-0.011 ± 0.009	0.044 ± 0.009	0.046	104 ± 11	3.7×10^{-6}
16 - 32	6,604	0.007 ± 0.017	0.050 ± 0.017	0.051	82 ± 20	0.014
≥ 32	1,513	-0.03 ± 0.04	0.05 ± 0.04	0.06	115 ± 35	0.26

Constant phase in spite of a (naturally) more limited significance of the amplitude

Dipole amplitude reconstruction

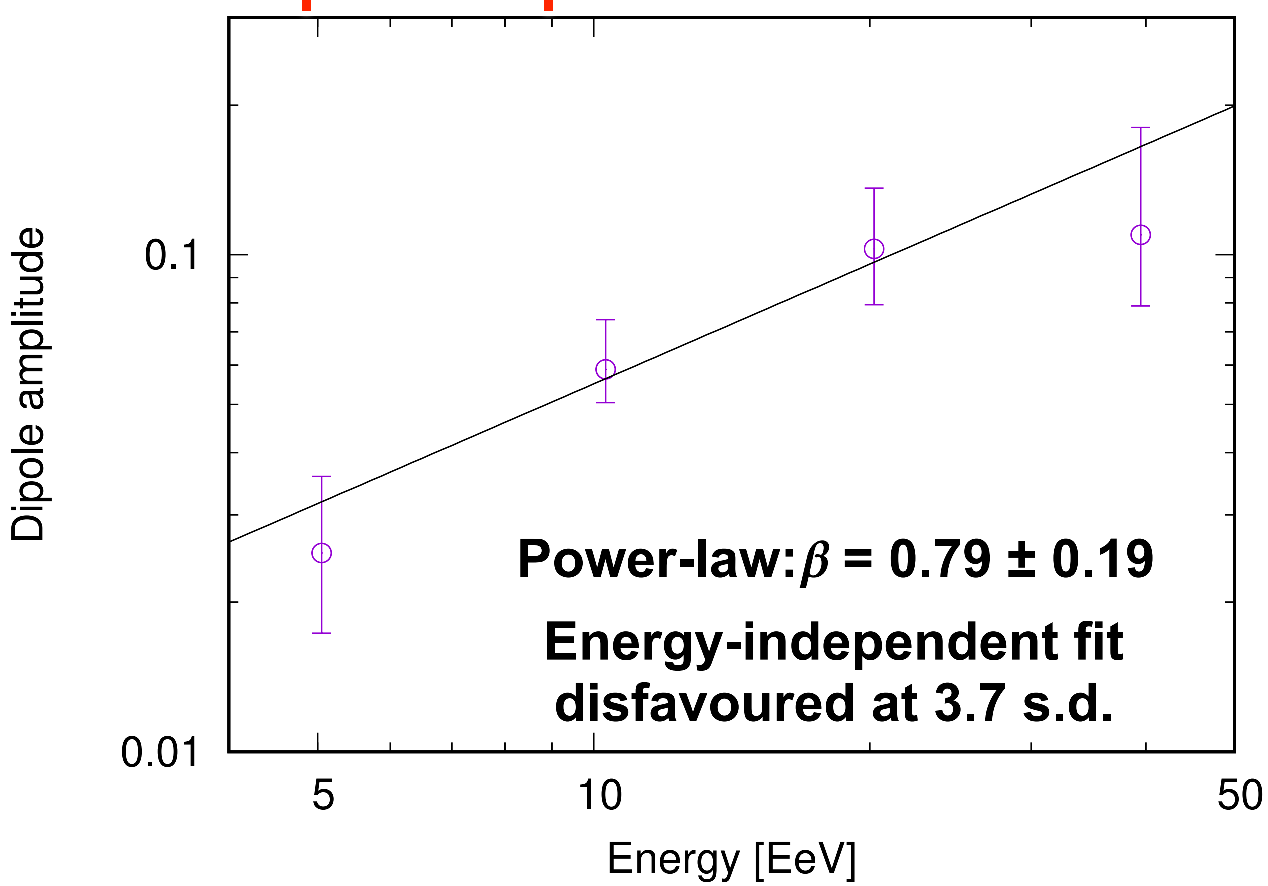

Indication of an increase of the dipole amplitude vs energy

Constant direction

Large-scale analysis: UHECRs and "close-by" galaxies

Amplitude: $6.5^{+1.3}_{-0.9}$%

Galactic longitude: 233˚, Galactic latitude: -13˚

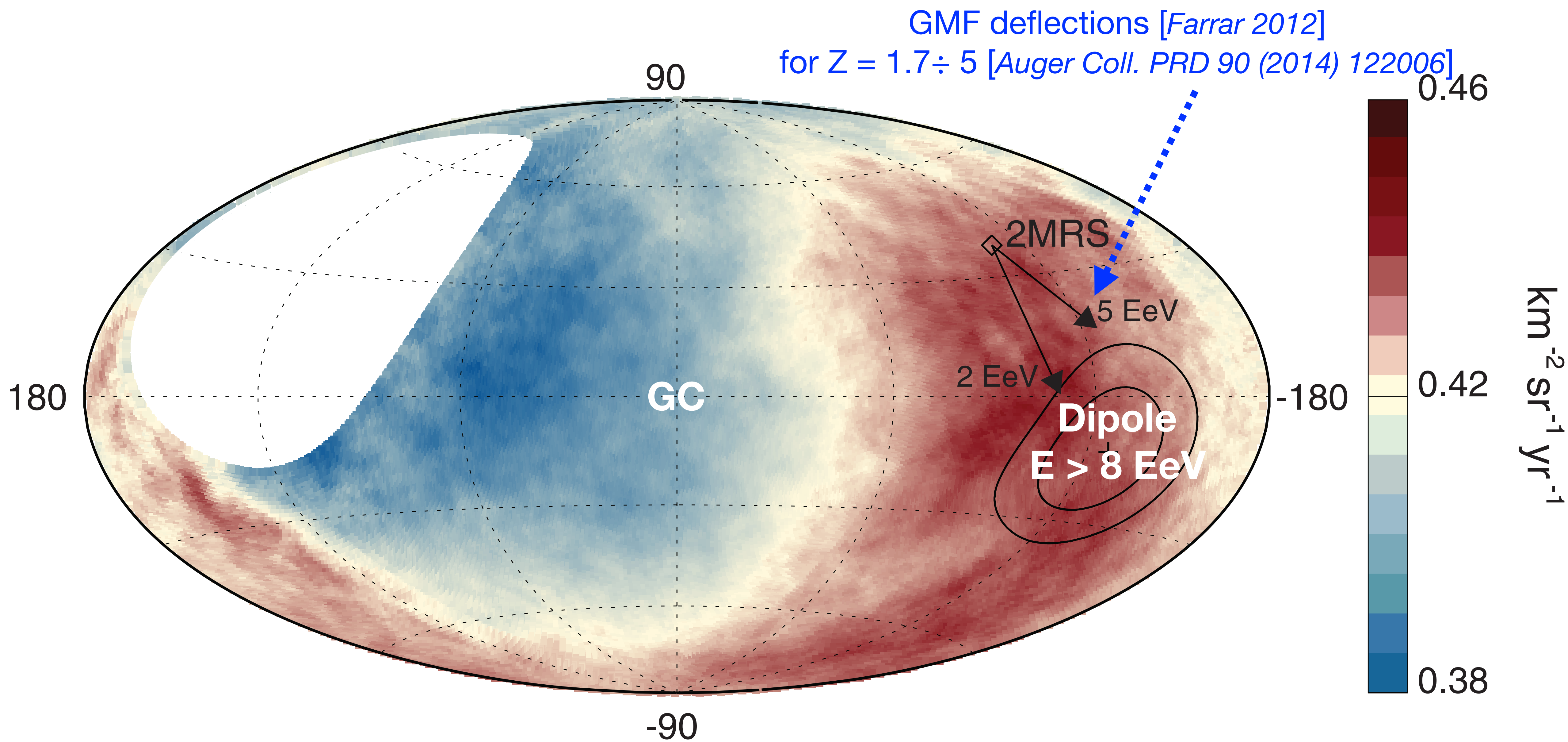

Amplitude: factor 10 > CG effect due to the Earth motion in the CR rest frame.

Larger anisotropies if sources distributed inhomogeneously or CRs diffused by IGMF.

Amplitudes depend on CR composition and source distributions

Appealing rapprochement of the CR dipole direction with that of 2MRS galaxies when CR compositions inferred at these energies are assumed

“Small”-scale analysis: UHECRs and “close-by" galaxies

The candidate galaxies and the analysis method

[Auger Coll. ApJL 853 (2018) L29]

γ-ray AGNs from the 2FHL catalog

(Fermi-LAT, E>50 GeV)

R < 250 Mpc

17 objects (among which Cen A, M87, Mkn 421, Mkn501…)

γ-ray flux used as proxy for the UHECR flux

γ-ray SBGs searched by Fermi-LAT

(from the HCN survey)

R < 250 Mpc

Radio-flux > 0.3 Jy

23 objects (among which M82, NGC253, and other 5 detected in γ)

Radio-flux used as proxy for the UHECR flux

Method: Unbinned maximum LH analysis

UHECR sky model: isotropy + anisotropic component from the sources

Directional exposure accounted

TS = LH ratio between H(UHECR sky model) and H(isotropy)

TS maximised vs search radius, ϑ, and anisotropic fraction, α

Test repeated over several energy thresholds (E > 20 EeV, up to E > 80 EeV, 1 EeV steps)

Flux attenuation accounted for at each energy threshold

Composition inferred by Auger data accounted for

"Small"-scale analysis: results

≈ 5500 UHECRs exploited (≈ 90000 km² sr y)

[Auger Coll. ApJL 853 (2018) L29]

AGNs

TS is maximum for E > 60 EeV (177 events)

SBGs

TS is maximum for E > 39 EeV (894 events)

TS as a function of energy threshold

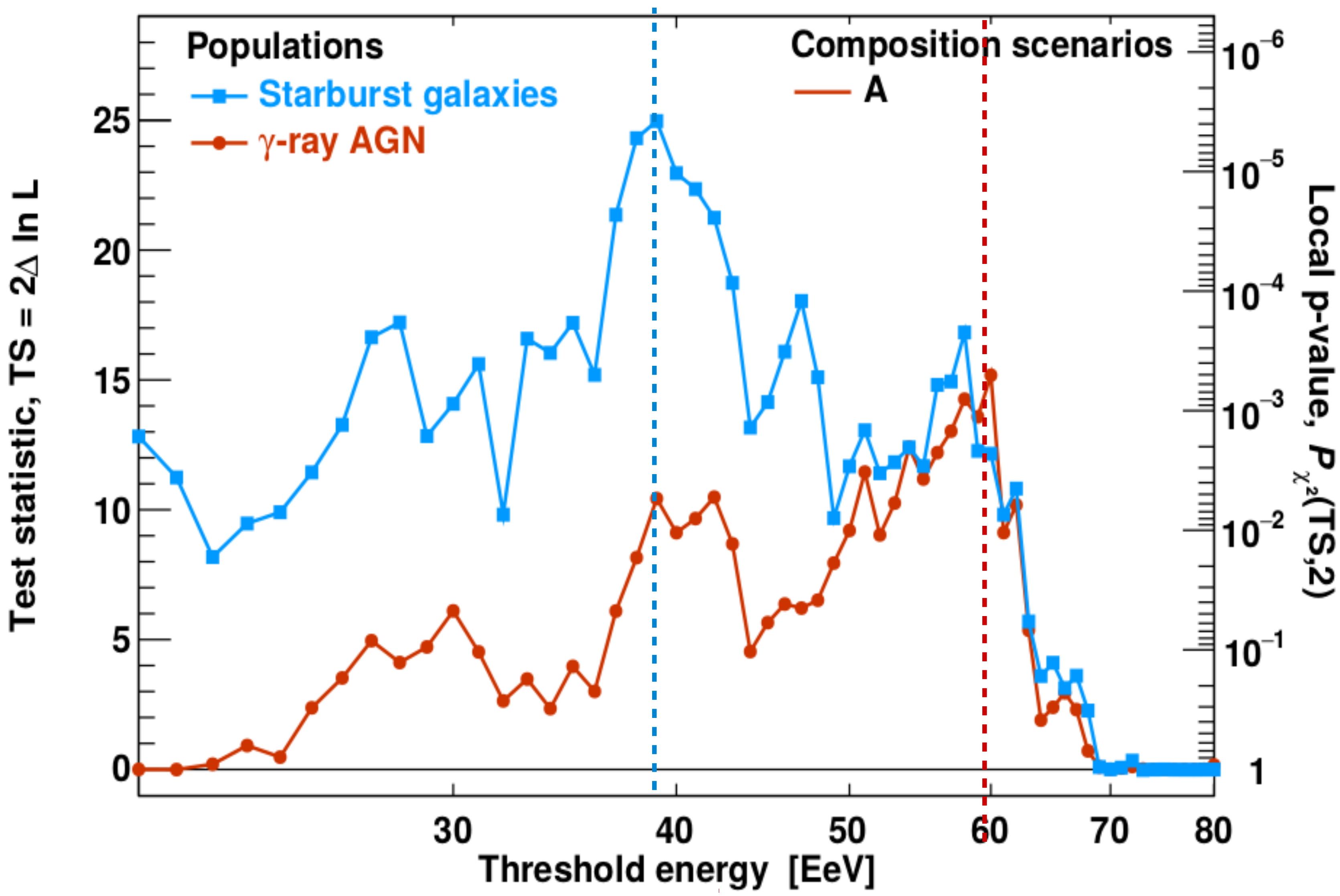

"Small"-scale analysis: results

≈ 5500 UHECRs exploited (≈ 90000 km² sr y)

[Auger Coll. ApJL 853 (2018) L29]

AGNs

TS is maximum for E > 60 EeV (177 events)

$\alpha = 7 \pm 4\%$, $\vartheta = 7^{\circ} \pm 4^{\circ}$

Post-trial (2 par. and E scan): 2.7 s.d.

SBGs

TS is maximum for E > 39 EeV (894 events)

$\alpha = 10 \pm 4\%$, $\vartheta = 13^{\circ} \pm 4^{\circ}$

Post-trial (2 par. and E scan): 4.0 s.d.

Maximum TS: radius and anisotropy fraction

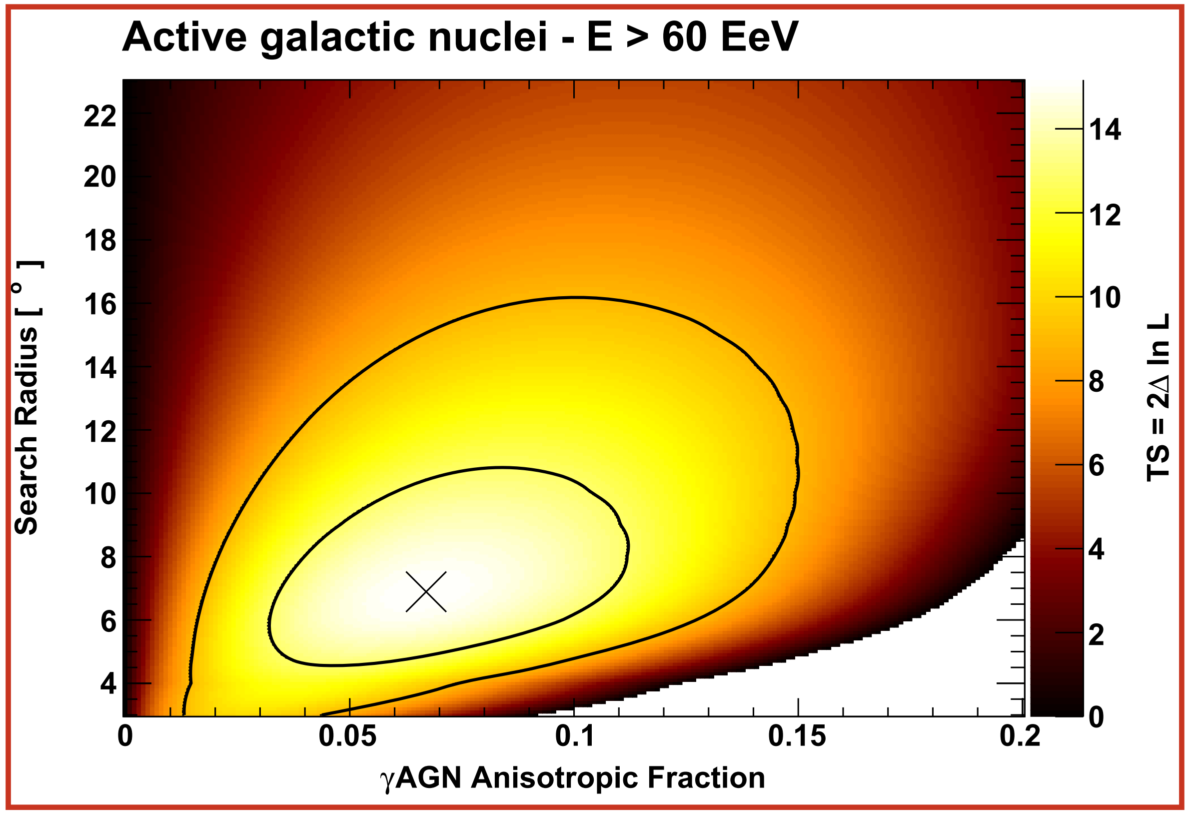

Maximum TS: radius and anisotropy fraction

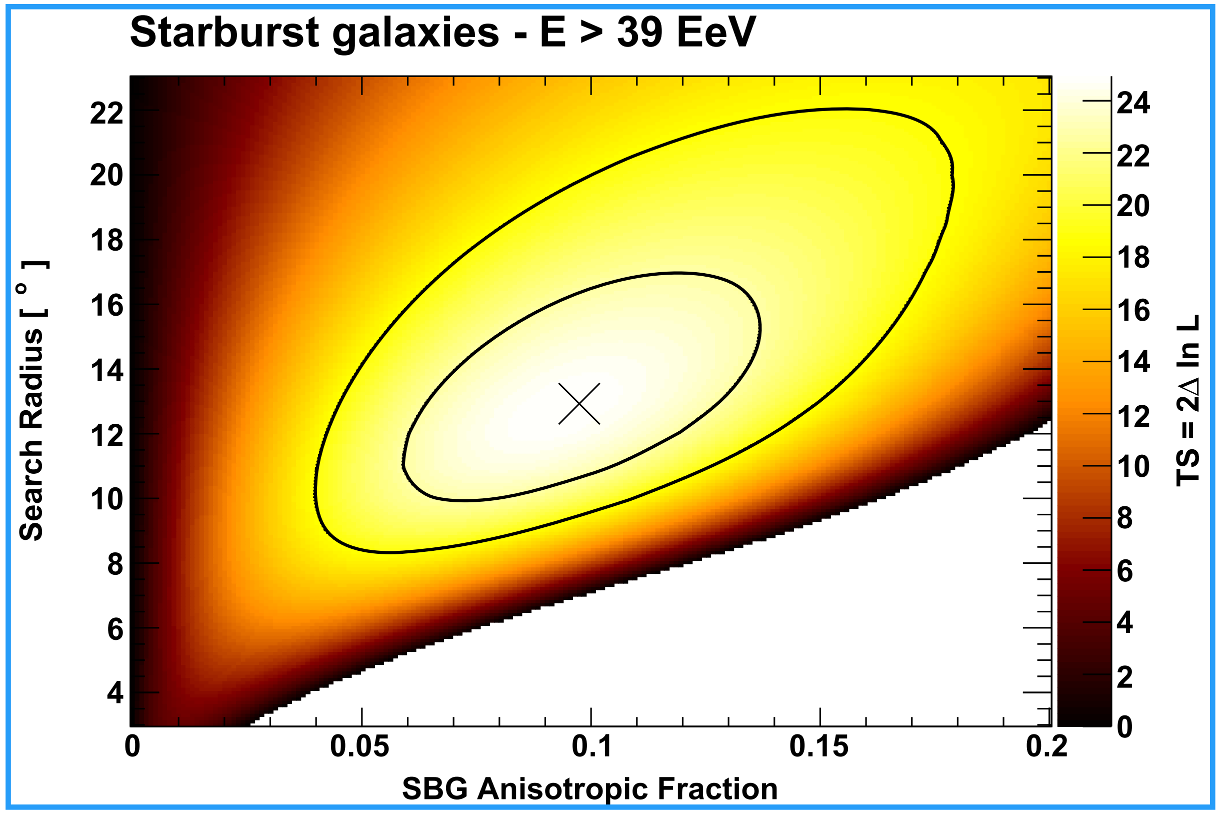

Comparison with SBGs indicates that isotropy is disfavoured with 4 s.d. significance (post-trial)

“Small”-scale analysis: other source models

Flux-limited samples of extra-galactic sources

[Auger Coll. ApJL 853 (2018) L29]

2MRS (infrared)

TS is maximum for E > 38 EeV

α = 7 ± 4%, ϑ = 12° ± 6°

Post-trial (2 par. and E scan): 2.7 s.d.

Swift-BAT (X-rays)

TS is maximum for E > 39 EeV

α = 16 ± 8%, ϑ = 13° ± 7°

Post-trial (2 par. and E scan): 3.2 s.d.

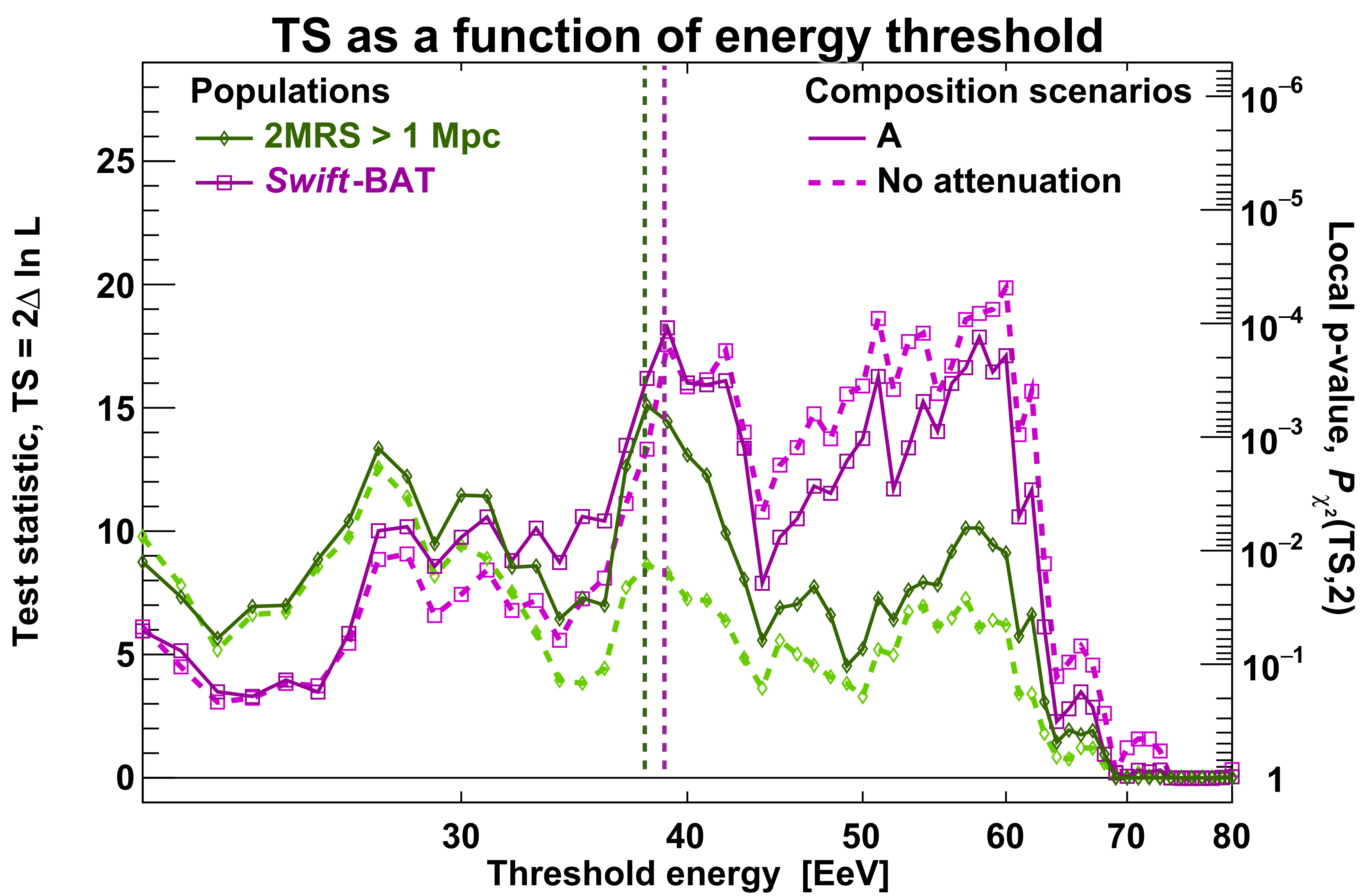

The contribution of SBGs to the indication of anisotropy remains larger than that of alternative catalogs tested

Conclusions (so far)

"…In the hope of finding clues to what extraordinary processes are capable of accelerating particles to such enormous energies, physicists would like to know whether the most energetic particles come from all directions or only from certain regions of the sky… [Bruno Rossi, 1964]"

"Large" scale studies

The most energetic particles do come with a preference from certain regions of the sky:

- **Discovery (> 5 s.d.) at E > 8 EeV** of a 4.7% anisotropy in α, with φ=100˚±10˚
- **Assuming a purely dipolar* anisotropy,** its amplitude is d = $6.5^{+1.3}_{-0.9}$% pointing at (α,δ)=(100˚, -24˚)
- The **direction** (> 100˚ from the GC) supports the hypothesis that CRs at these energies are **extragalactic**
- The **amplitude** is much larger than expected from a motion-origin (CG), hinting at a **"source-origin"**

"Small" scale studies

We might have found some clues on what extraordinary processes might accelerate particles to such enormous energies:

- **Indication (4 s.d.) at 39 EeV** of an anisotropy at intermediate scales (≈ 13˚) in association with **Starburst Galaxies**
- **Smaller indication** when studying other source catalogs (AGNs, 2MRS, Swift-BAT) tested
- Caveat on significance: numerous studies have been done on our data, public in part.
- Further caveat: effects due to GMF and EGMF not included. Primary mass not probed (yet) about 40 EeV

* Assuming a dipole+quadrupole, none of the quadrupole components is statistically significant [arXiv 1808.03579]

Next?

- **Large and "small" scales: keep collecting data (and controlling them ;-).** Higher order multipoles? Confirm the SBGs-based anisotropy? Relate large to intermediate angular scales?
- **Large scales: go to lower energies,** to probe the Galactic-to-extragalactic transition. Work in progress to update and extend our first study (APP 34, 2011, 627)
- **Large and "small" scales: go to full sky** (with Telescope Array, see Jonathan Biteau's report of the joint Auger/TA WG)
- **Large and "small" scales: mass-discrimination criteria** in anisotropy analyses. AugerPrime (see Antonella Castellina's talk on Friday)

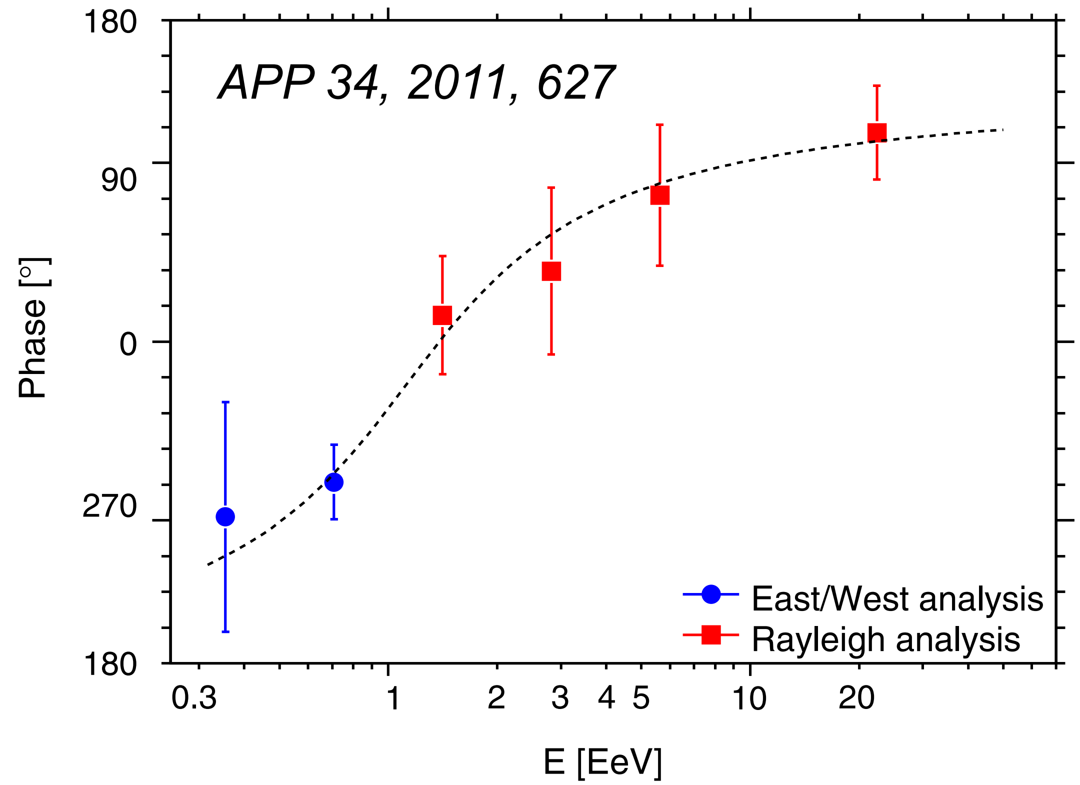

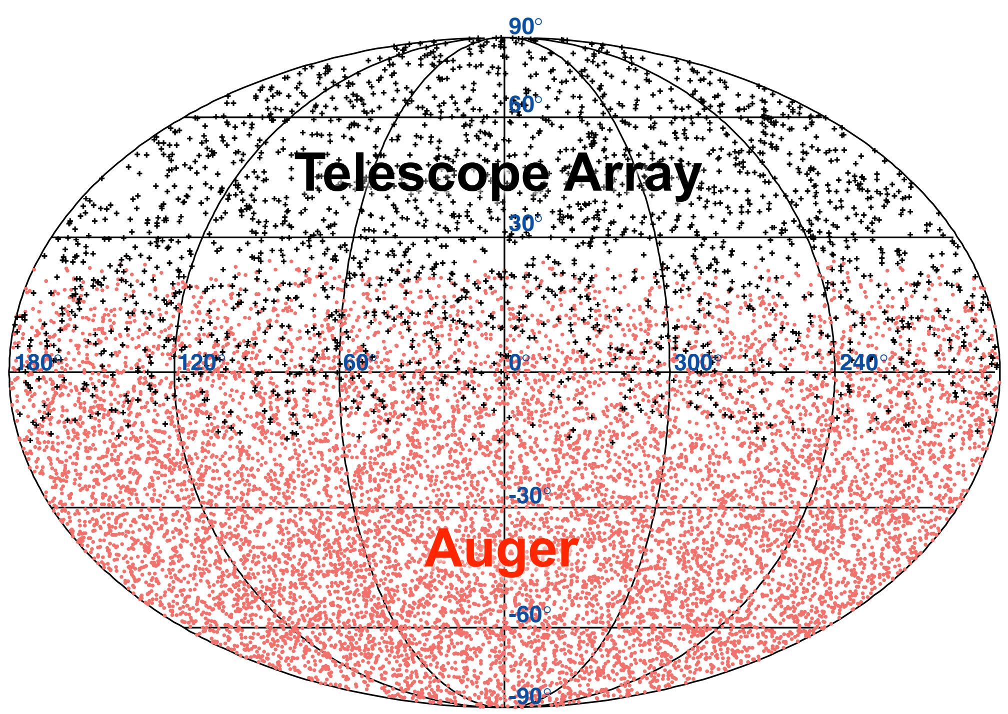

ApJ 794, 2014, 172

Backup

Chance probability in harmonic analysis

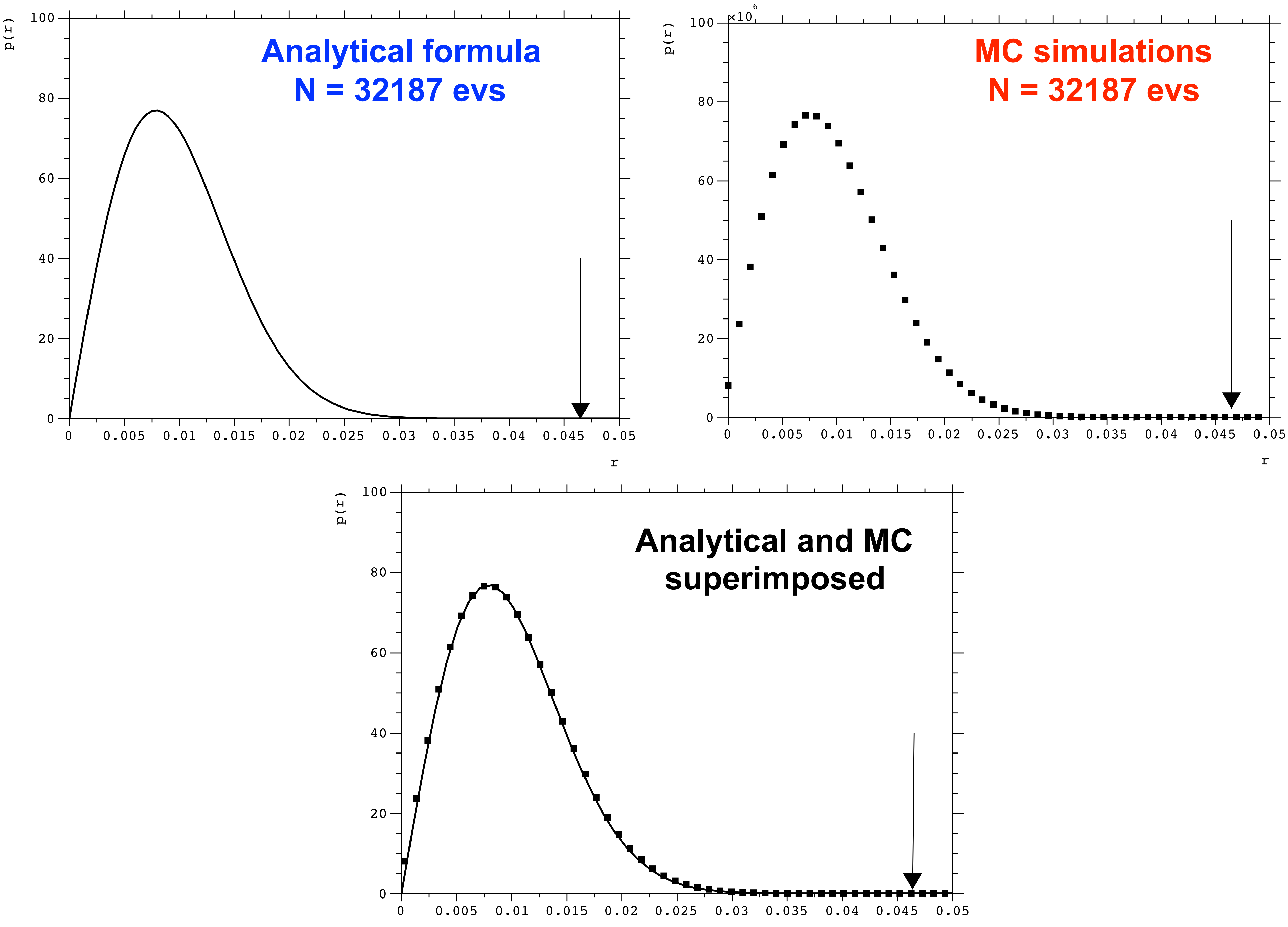

I and II harmonic analysis in azimuth

[Auger Coll. arXiv 1808.03579, just accepted by ApJ]

Energy [EeV]	k	a_k^ϕ	b_k^ϕ	$P(\geq\mid a_k^\phi \mid)$	$P(\geq\mid b_k^\phi \mid)$
4 - 8	1	-0.010 ± 0.005	-0.013 ± 0.005	0.045	0.009
	2	0.002 ± 0.005	-0.002 ± 0.005	0.69	0.69
$\geq$ 8	1	-0.007 ± 0.008	-0.014 ± 0.008	0.38	0.08
	2	-0.002 ± 0.008	0.006 ± 0.008	0.80	0.45

Large-scale anisotropies expected from Galactic CRs

[Auger Coll. arXiv 1808.03579, just accepted by ApJ]

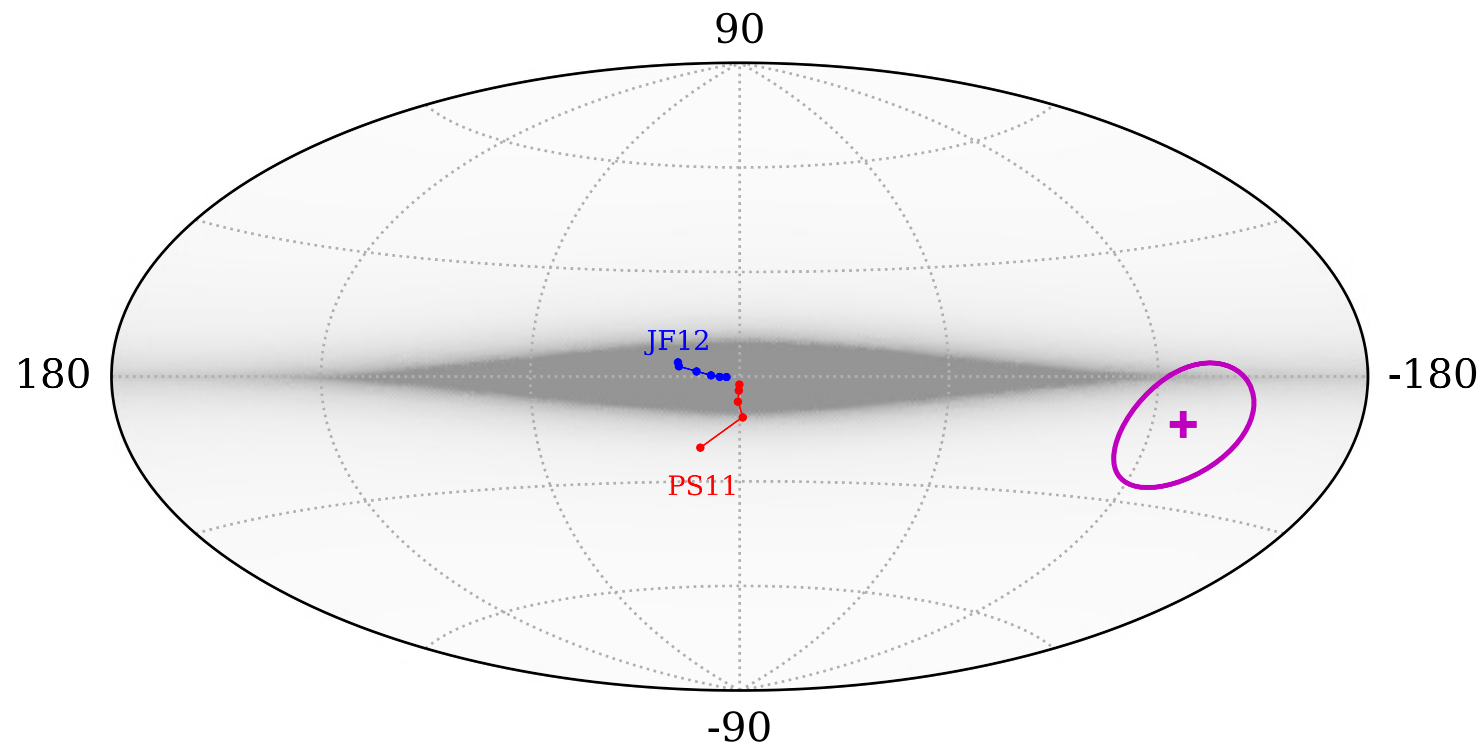

Figure 5. Map in Galactic coordinates of the direction of the dipolar component of the flux for different particle rigidities for cosmic rays coming from Galactic sources and propagating in the Galactic magnetic-field model of Jansson & Farrar (2012) (blue points) and the bisymmetric model of Pshirkov et al. (2011) (red points). The points show the results for the following rigidities: 64 EV, 32 EV, 16 EV, 8 EV, 4 EV and 2 EV (with increasing distance from the Galactic center). We also show in purple the observed direction of the dipole for $E \geq 8$ EeV and the 68% CL region for it. The background in gray indicates the integrated matter density profile assumed for the Galactic source distribution (Weber & Boer 2010).

Harmonic analysis vs energy

Splitting the E>8 bin in three

Auger Coll. arXiv 1808.03579, just accepted by ApJ]

Right ascension

Energy [EeV]	events	a_1^α	b_1^α	r_1^α	φ_1^α [°]	$P(\geq r_1^\alpha)$
8 - 16	24,070	-0.011 ± 0.009	0.044 ± 0.009	0.046	104 ± 11	3.7×10^{-6}
16 - 32	6,604	0.007 ± 0.017	0.050 ± 0.017	0.051	82 ± 20	0.014
≥ 32	1,513	-0.03 ± 0.04	0.05 ± 0.04	0.06	115 ± 35	0.26

Azimuth

Energy [EeV]	a_1^ϕ	b_1^ϕ	$P(\geq \lvert a_1^\phi \rvert)$	$P(\geq \lvert b_1^\phi \rvert)$
8 - 16	-0.013 ± 0.009	-0.004 ± 0.009	0.15	0.66
16 - 32	0.003 ± 0.017	-0.042 ± 0.017	0.86	0.013
≥ 32	0.05 ± 0.04	-0.04 ± 0.04	0.21	0.32

Dipole reconstruction vs energy

[Auger Coll. arXiv 1808.03579, just accepted by ApJ]

Energy [EeV] interval	median	$d_\perp$	d_z	d	α_d [°]	δ_d [°]
4 - 8	5.0	$0.006^{+0.007}_{-0.003}$	-0.024 ± 0.009	$0.025^{+0.010}_{-0.007}$	80 ± 60	-75^{+17}_{-8}
≥ 8	11.5	$0.060^{+0.011}_{-0.010}$	-0.026 ± 0.015	$0.065^{+0.013}_{-0.009}$	100 ± 10	-24^{+12}_{-13}
8 - 16	10.3	$0.058^{+0.013}_{-0.011}$	-0.008 ± 0.017	$0.059^{+0.015}_{-0.008}$	104 ± 11	-8^{+16}_{-16}
16 - 32	20.2	$0.065^{+0.025}_{-0.018}$	-0.08 ± 0.03	$0.10^{+0.03}_{-0.02}$	82 ± 20	-50^{+15}_{-14}
≥ 32	39.5	$0.08^{+0.05}_{-0.03}$	-0.08 ± 0.07	$0.11^{+0.07}_{-0.03}$	115 ± 35	-46^{+28}_{-26}

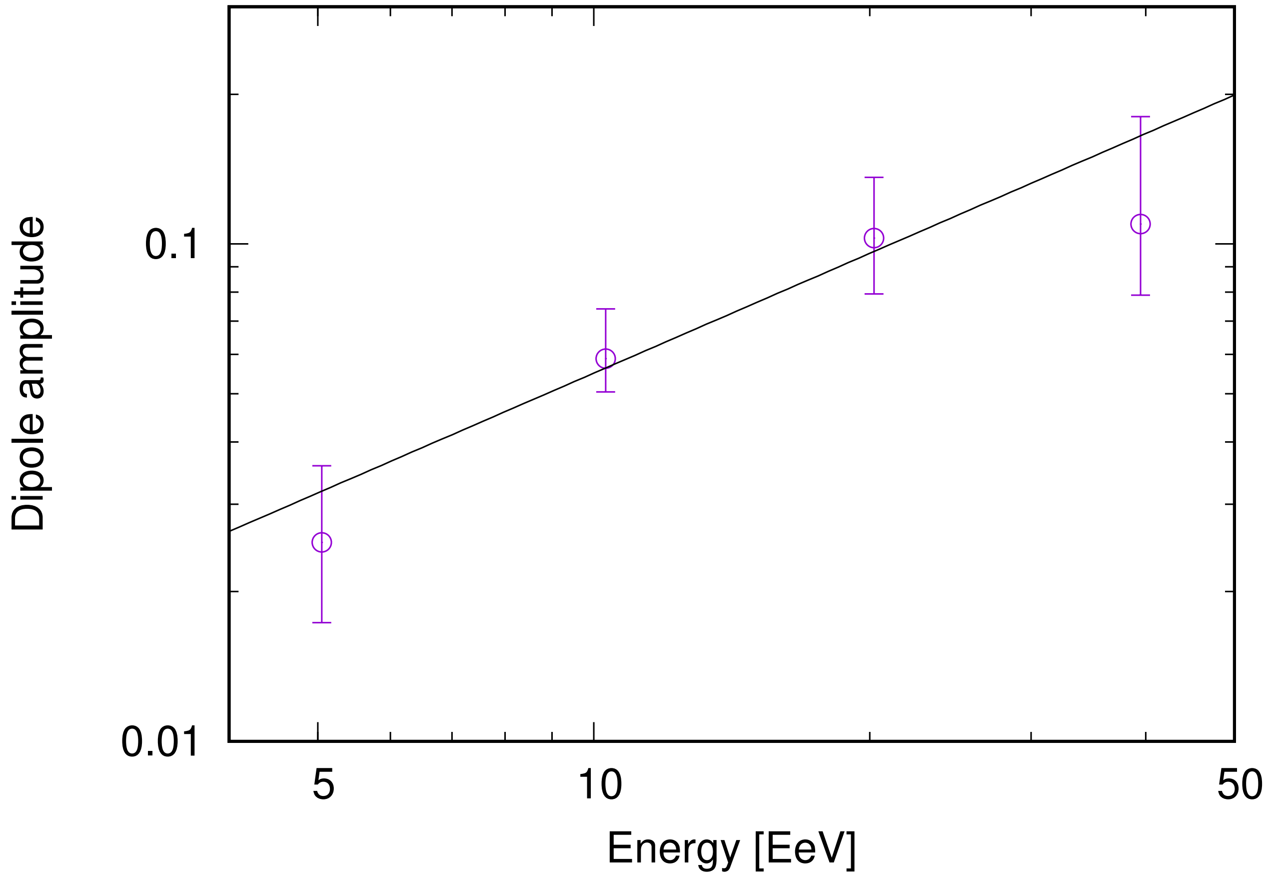

Maximum likelihood fit

Power-law index β = 0.79 ± 0.19

Energy-independent fit disfavoured at 3.7 s.d.

Dipole reconstruction vs energy

[Auger Coll. arXiv 1808.03579, just accepted by ApJ]

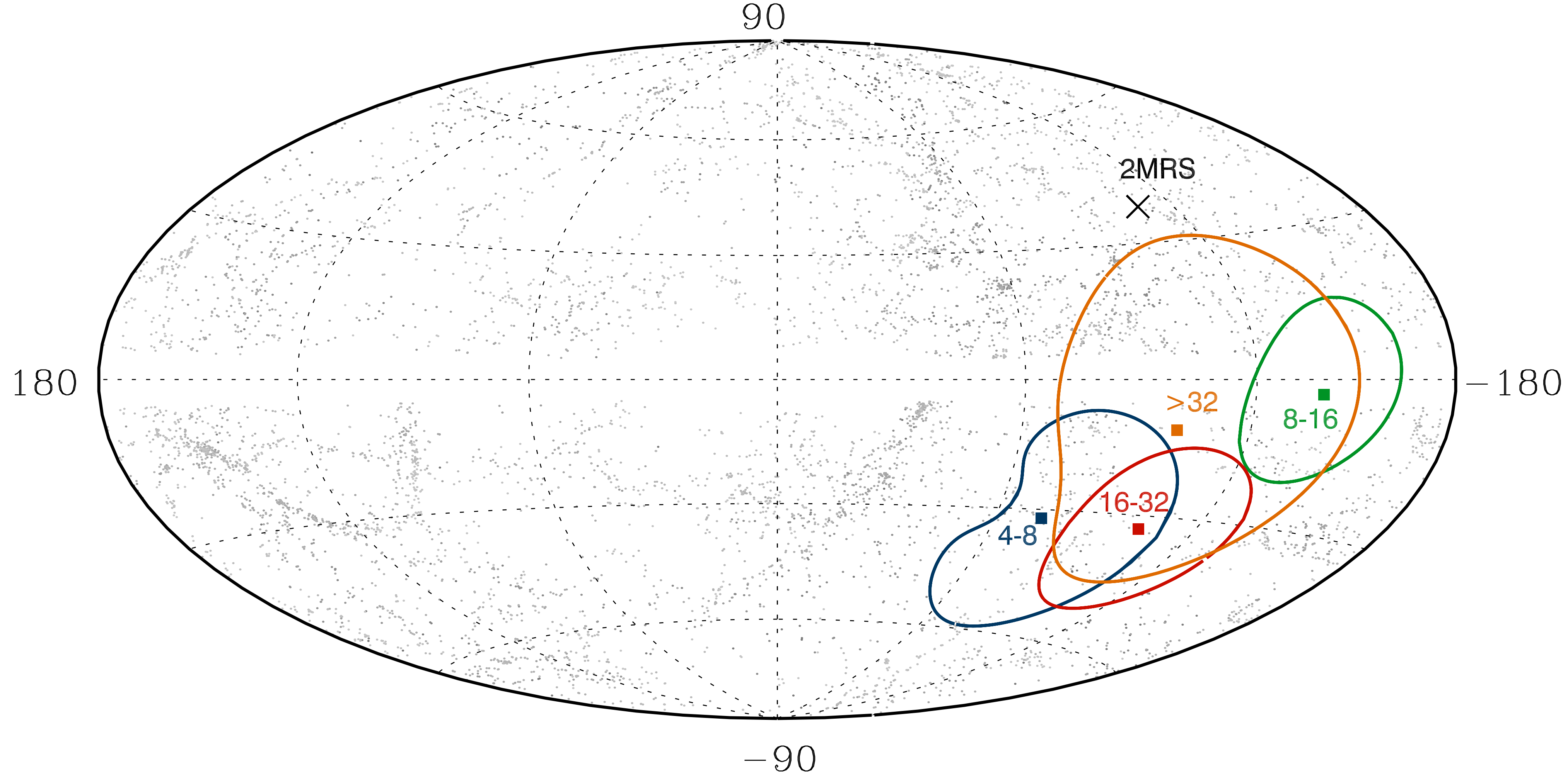

Reconstruction of dipole + quadrupole

[Auger Coll. arXiv 1808.03579, just accepted by ApJ]

Energy [EeV]	d_i	Q_{ij}
4 - 8	$d_x = -0.005 \pm 0.008$	$Q_{zz} = -0.01 \pm 0.04$
	$d_y = 0.005 \pm 0.008$	$Q_{xx} - Q_{yy} = -0.007 \pm 0.029$
	$d_z = -0.032 \pm 0.024$	$Q_{xy} = 0.004 \pm 0.015$
		$Q_{xz} = -0.020 \pm 0.019$
		$Q_{yz} = -0.005 \pm 0.019$
≥ 8	$d_x = -0.003 \pm 0.013$	$Q_{zz} = 0.02 \pm 0.06$
	$d_y = 0.050 \pm 0.013$	$Q_{xx} - Q_{yy} = 0.08 \pm 0.05$
	$d_z = -0.02 \pm 0.04$	$Q_{xy} = 0.038 \pm 0.024$
		$Q_{xz} = 0.02 \pm 0.03$
		$Q_{yz} = -0.03 \pm 0.03$

None of the quadrupole components is statistically significant

Reconstructed dipole consistent with those obtained under the pure-dipole assumption

Sky maps

SBGs

Observed Excess Map - E > 39 Eev

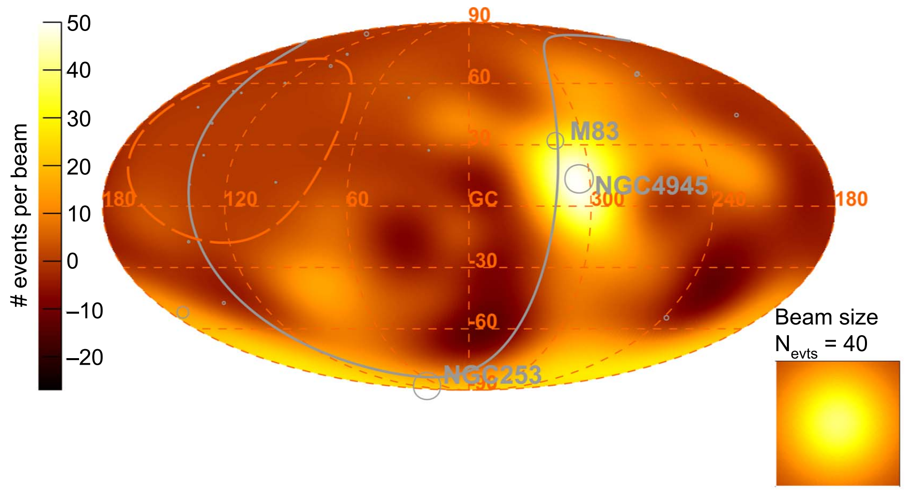

Model Excess Map - Starburst galaxies - E > 39 EeV

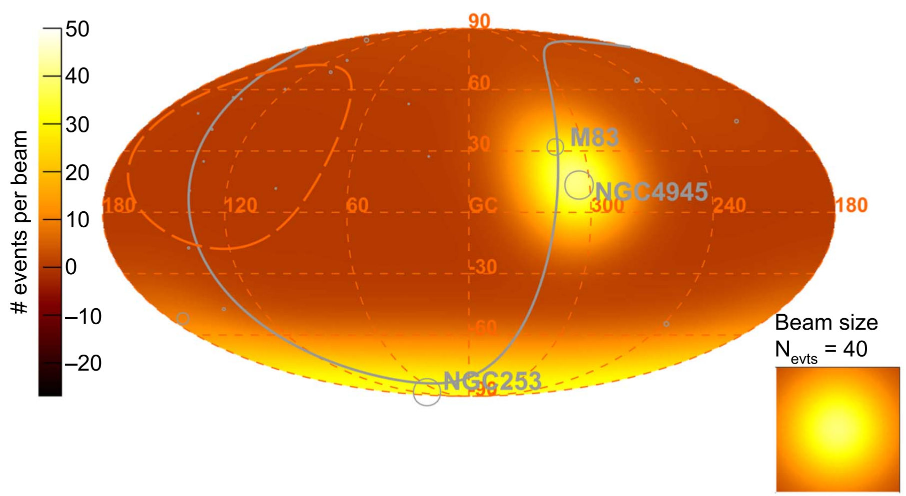

Residual Excess Map - Starburst galaxies - E > 39 EeV

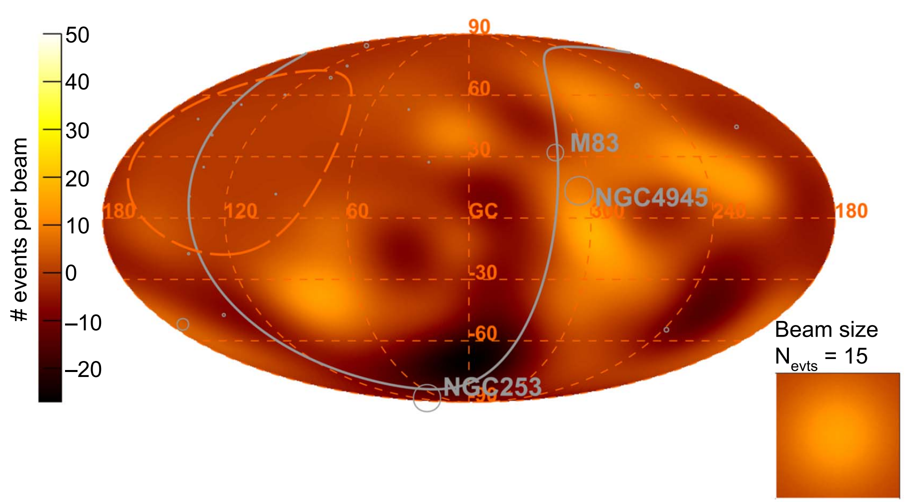

AGNs

Observed Excess Map - E > 60 Eev

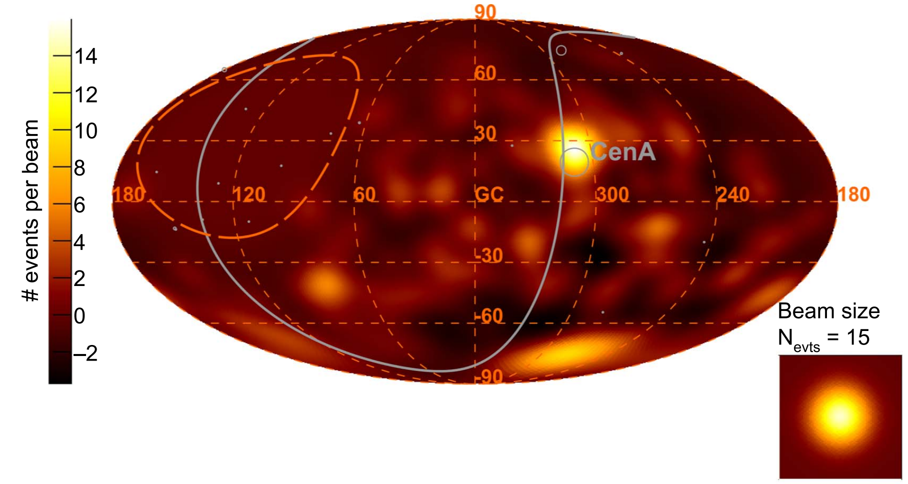

Model Excess Map - Active galactic nuclei - E > 60 EeV

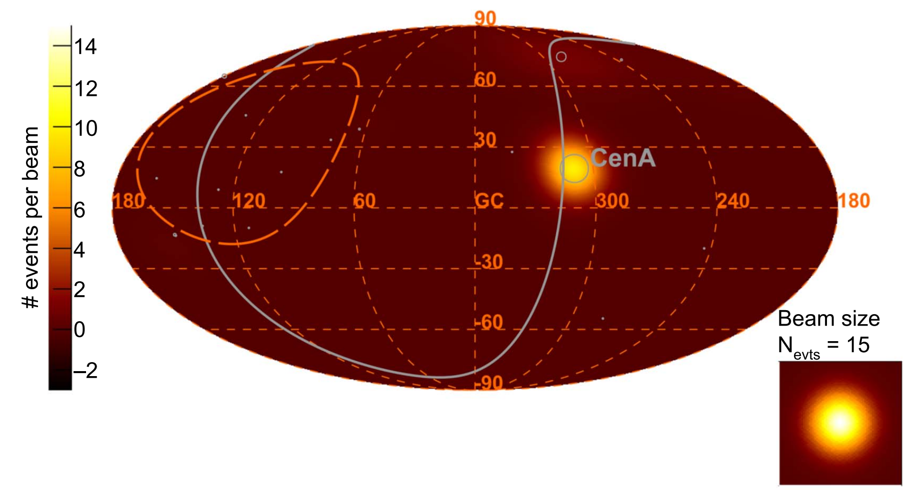

Residual Excess Map - Active galactic nuclei - E > 60 EeV

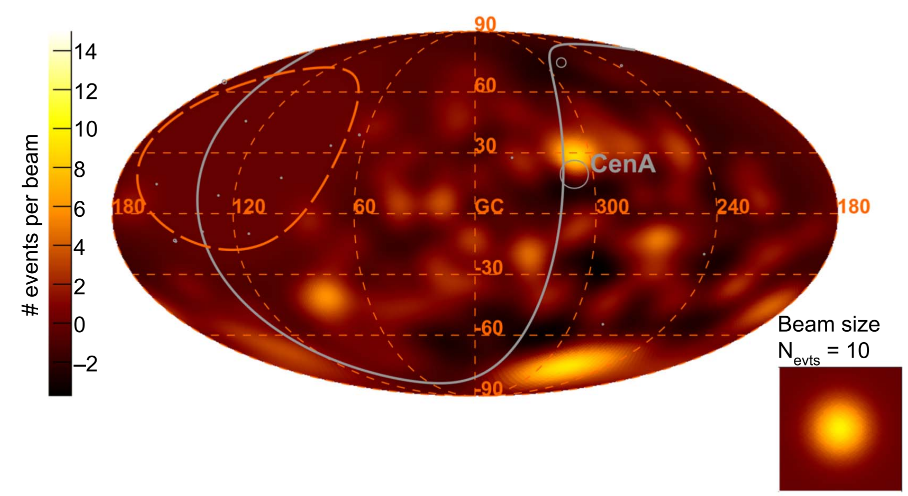

SBGs Test Statics vs time